

# Design of a 45-degree Linearly-polarized Hollow-waveguide Slot Two-dimensional Array Antenna with a Full-corporate-feed Circuit in the Lower Layer

<sup>#</sup>Takashi Tomura<sup>1</sup>, Yohei Miura<sup>1</sup>, Miao Zhang<sup>1</sup>, Jiro Hirokawa<sup>1</sup>, Makoto Ando<sup>1</sup>

<sup>1</sup>Dept. of Electrical and Electronic Eng., Tokyo Institute of Technology

2-12-1-S3-19, O-okayama, Meguro-ku, Tokyo, 152-8552, JAPAN

E-mail: tomura@antenna.ee.titech.ac.jp

## 1. Introduction

Hollow-waveguide slot array antennas [1] have been widely used in the milli-meter band since they do have neither radiation loss nor dielectric loss. Furthermore, they have been developed especially for military application such as radars. For commercial application such as fixed wires access system, mass production at low cost has been required and single layer hollow-waveguide slot array antennas [2] [3] have been developed to solve the problem. However, the bandwidth of gain is narrow due to the series feed and the long-line effect. To prevent the narrow bandwidth of gain, center-feed structure [4] and partially corporate feed structure [5] have been proposed. The bandwidth of gain was improved but increase of a blocking area leads to low aperture efficiency. The structure of the double-layer corporate-feed waveguide slot array [6] was proposed to achieve the wide bandwidth of gain and the high aperture efficiency. It can be mass-produced at low cost by diffusion bonding of laminated thin metal plates [7]. In this paper, we propose a 45-degree linearly-polarized configuration, placing inclined slots on a double-layer full-corporate-feed hollow-waveguide slot array antenna and design 4-element sub-array.

## 2. Configuration and Operation of the Antenna

Figure 1 shows the proposed 45-degree linearly-polarized hollow-waveguide slot array antenna with full-corporate feed. Figure 2 shows the exploded perspective view of a 4-element array. The antenna is composed of the feeding part in the lower layer and the radiating part in the upper layer. The feeding circuit is a full-corporate feed and a combination of H-plane T-junctions. The radiating part is fed through a coupling aperture located at the feeding circuit terminal. 45-degree inclined radiating slots are placed on exciting slots. Six etching patterns such as the radiating slots, the exciting slots, the cavities, the coupling apertures, the feeding circuit and the feeding aperture, are required for fabrication by diffusion bonding.

## 3. Design of 256-element array

### 3.1 Design of 4-element sub-array

Figure 3 shows an analysis model of the 4-element sub-array. Two pairs of periodic boundary walls are assumed to take into account mutual coupling among the sub-arrays infinitely arrayed two-dimensionally. The design frequency is 61.5 GHz. The width of the radiating and exciting slots is 2.74 mm, the exciting slot width is 1.75 mm, the radiating slot width is 0.75 mm and the element spacing is 4.20 mm.

Figure 4 shows the cross polarization as a function of the radiating slot width. The cross polarization is suppressed up to  $-30$  dB when the radiating slot width is less than 0.9 mm. The length of the walls in the cavity is adjusted for impedance matching. The frequency characteristics of reflection are shown in Figure 5. The fractional bandwidth for reflection less than  $-14$  dB is 5.9 % and it is less than the fractional bandwidth (9.1 %) of the model without the radiating slots [8]. However, double resonances are obtained as same as the model without the radiating slots.

### 3.2 Analysis of 256-element array

A 256-element array composed of the designed 4-element sub-arrays and the full-corporate-feed circuit [6] are analysed. The aperture dimension of the antenna is  $67.2 \text{ mm} \times 67.2 \text{ mm}$ .

The reflection of the 256-element array and the feeding circuit are shown in Figure 5. The reflection is almost equivalent to that of the 4-element sub-array though it has ripples caused by the reflection of the feeding circuit. The fractional bandwidth is 4.2 % and it is less than that of the 4-element sub-array because it is influenced by the reflection of the feeding circuit. It is predictable that the frequency characteristic of the reflection of the 256-element array is improved when that of the feeding circuit is improved. The frequency characteristic of the cross polarization in the boresite ( $\theta=0$ ) is shown in Figure 6. The cross polarization is less than  $-30 \text{ dB}$  over the bandwidth. The directivity and the aperture efficiency are shown in the same figure.  $32.9 \text{ dBi}$  directivity with 82 % aperture efficiency is obtained at  $61.5 \text{ GHz}$ . The radiation pattern on the E-plane is shown in Figure 7. The first sidelobe level is low,  $-26 \text{ dB}$ ; however,  $-16 \text{ dB}$  grating lobes are generated in  $\pm 55$ -degree directions. This grating lobe generation results from amplitude and phase difference among the radiation slots and is discussed in the next chapter.

## 4. Effects by Amplitude and Phase difference

Magnetic field lines without the radiating slots are shown in Figure 8. The magnetic field lines are symmetrical with respect to the y-z and z-x planes because the configuration of the cavity and the exciting slots has also this symmetry. Thus, the exciting slots are fed with equal amplitude and phase. However, when the radiating slots are placed on the exciting ones, the configuration breaks this symmetry and the magnetic field lines also become asymmetry. The configuration has point symmetry with respect to the origin on the x-y plane and two radiating slots in the diagonal direction in the cavity are excited with equal amplitude and phase. However, neighbor slots placed parallel to the x and y-axis are excited with amplitude and phase difference. This causes generation of grating lobes on  $\phi = \pm 45^\circ$  plane. The amplitude and phase difference are denoted as  $\alpha$  and  $\beta$  respectively and 256-element array factor of point sources are calculated. The amplitude and phase difference of electric field on the radiating slots is  $2.5 \text{ dB}$  and  $11 \text{ degrees}$ , respectively by HFSS. 256-element array factor with those differences is shown in Figure 7 and it agrees with the radiation pattern well. The maximum value distribution of the grating lobes is shown in Figure 8. To suppress the grating lobes up to the first sidelobe level, it is required that amplitude and phase difference is less than  $0.9 \text{ dB}$  and  $6 \text{ degrees}$ .

To reduce the amplitude and phase difference, the exciting slots have to be excited uniformly. Thus, the exciting slot thickness is increased so that it cuts off higher order modes and propagates only the dominant mode and the differences are reduced as shown in Figure 10. The maximum value of the grating lobe is  $-25 \text{ dB}$ ,  $-37 \text{ dB}$  for  $1.2 \text{ mm}$  and  $2.4 \text{ mm}$  thickness respectively as shown in Figure 11. Next, impedance is matched by adjusting the length of the walls in the cavity when the thickness of the radiating slot is  $1.2 \text{ mm}$  and  $2.4 \text{ mm}$ . The fractional bandwidth of reflection is  $2.9 \%$  and  $3.1 \%$  for  $1.2 \text{ mm}$  and  $2.4 \text{ mm}$  thickness respectively as shown in Figure 12. Those are less than  $5.9 \%$ ; the fractional bandwidth for  $0.3 \text{ mm}$  thickness.

As a result, we find trade-off relationship between the grating lobe level and the bandwidth.

## 5. Conclusion

We have proposed the 45-degree linearly-polarized hollow-waveguide slot array antenna with full-corporate feed. We have confirmed that the cross polarization is suppressed by the radiation slot width by the analysis of the 4-element sub-array. Amplitude and phase difference between neighbor slots generate the grating lobes. To suppress the grating lobes, the thickness of the exciting slots is increased and the grating lobes are reduced less than  $-37 \text{ dB}$ . However, as the thickness of the exciting slots increases, the bandwidth of reflection gets narrower and trade-off relationship between the grating lobe level and the bandwidth is found.

## References

- [1] R. C. Johnson, and H. Jasik, *Antenna Engineering Handbook*, New York: McGraw-Hill, 1984, Chap.9.
- [2] N. Goto, "A Planar Waveguide Slot Antenna of Single Layer Structure," IEICE Tech. Rept., AP88-39, 1988. (in Japanese)
- [3] N. Goto, "A Waveguide-Fed Printed Antenna," IEICE Tech. Rept., AP89-3, 1989.
- [4] S. Park, Y. Tsunemitsu, J. Hirokawa and M. Ando, "Center Feed Single Layer Slotted Waveguide Array," *IEEE Trans. Antennas Propag.*, vol.54, no.5, pp.1474-1480, May 2006.
- [5] S. Fujii, Y. Tsunemitsu, G. Yoshida, N. Goto, M. Zhang, J. Hirokawa and M. Ando, "A Wideband Single-layer Slotted Waveguide Array with an Embedded Partially Corporate Feed," ISAP2008, Session: TP-C27, Taiwan, Oct. 2008.
- [6] Y. Miura, J. Hirokawa, M. Ando, Y. Shibuya, G. Yoshida, "60GHz-band Fabrication of a Double-layer Corporate-feed Hollow-waveguide Slot Array by Diffusion Bonding of Laminated Thin Metal Plates," IEICE Gen. Conf. '10, BS-1-9, March 2010. (in Japanese)
- [7] M. Zhang, J. Hirokawa, M. Ando, "Fabrication of a Slotted Waveguide Array at 94GHz by Diffusion Bonding of Laminated Thin Plates," IEICE Tech. Rept., AP2008-35, June 2008. (in Japanese)
- [8] Y. Miura, J. Hirokawa, M. Ando, "Bandwidth Enhancement of a Double-layer Corporate-feed Hollow-waveguide Slot Array Antenna in 60 GHz-Band," IEICE Tech. Rept., AP2008-35, 2008-6. (in Japanese)

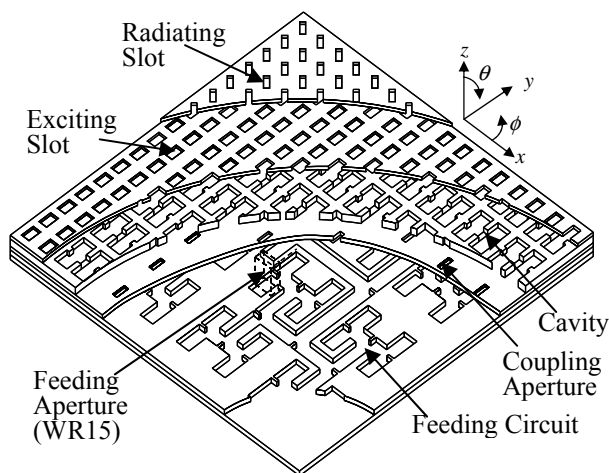


Figure 1: 45-degree linearly-polarized hollow-waveguide slot array antenna with full-corporate feed

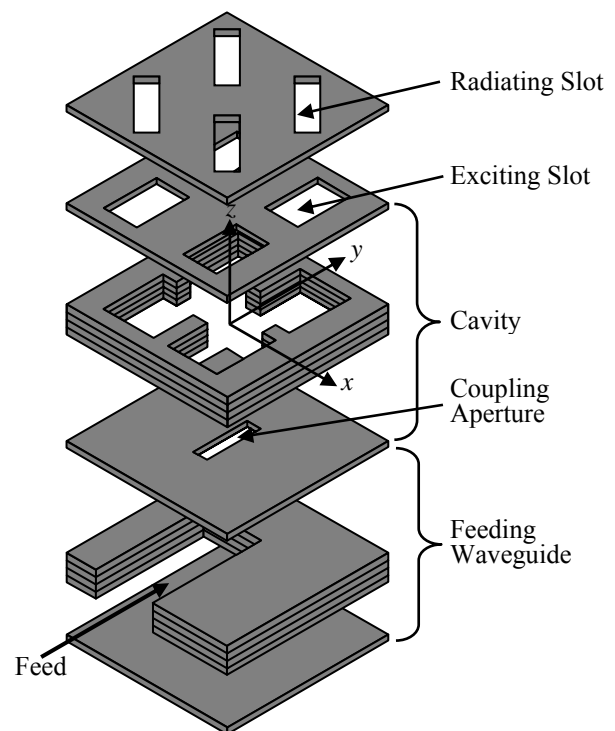


Figure 2: Exploded perspective view of the 4-element array

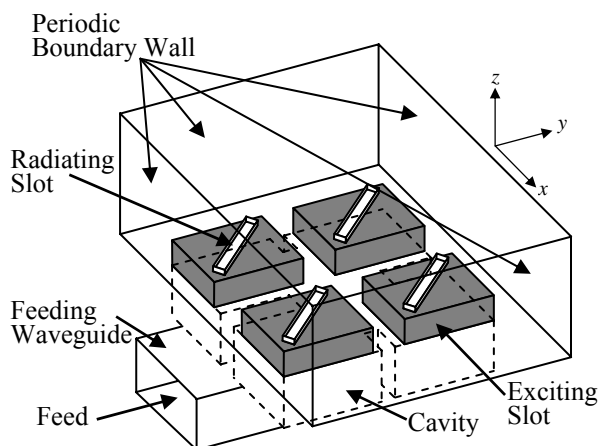


Figure 3: Analysis model of the 4-element array

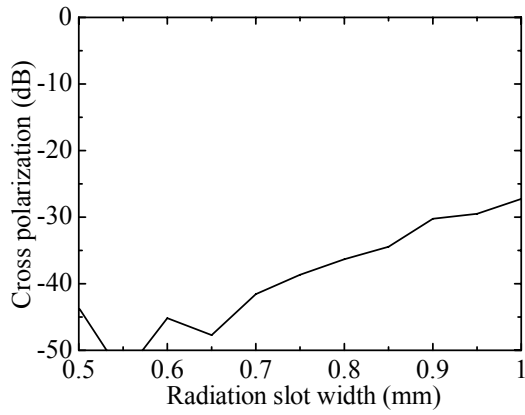


Figure 4: Cross polarization and directivity

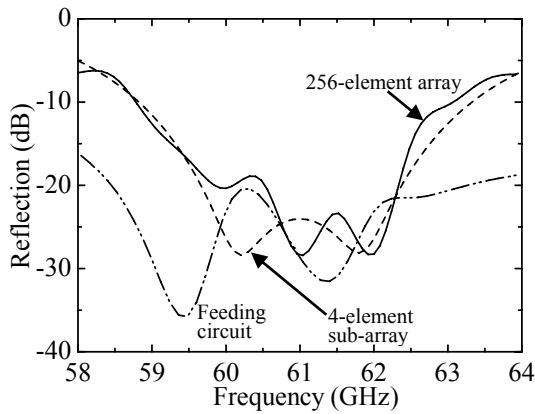


Figure 5: Reflection of 4-element sub-array, 256-element array and feeding circuit

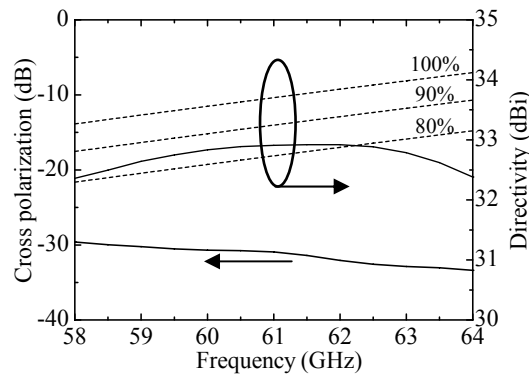


Figure 6: Cross polarization and directivity

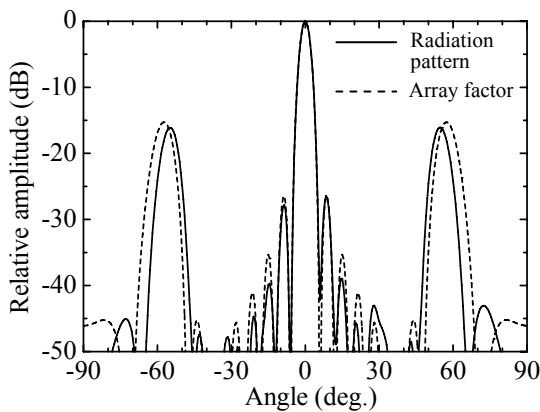


Figure 7: Radiation pattern of 256-element array on E-plane

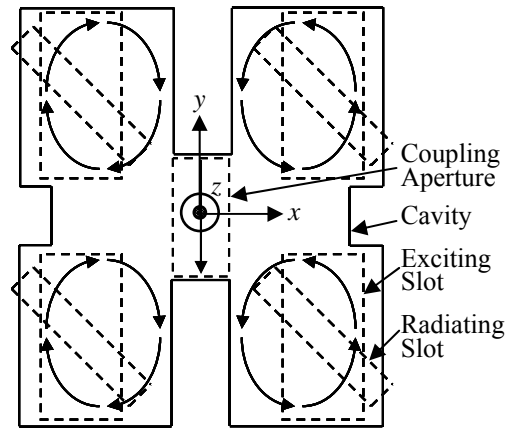


Figure 8: Magnetic field lines in the cavity

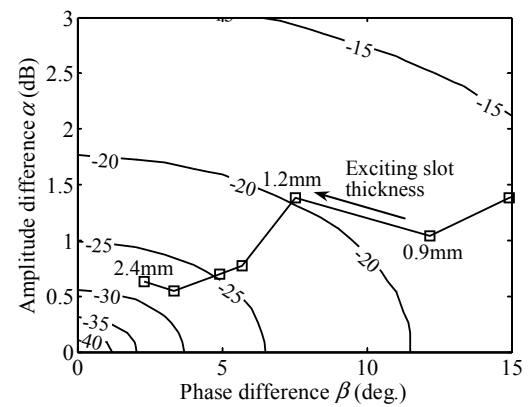


Figure 9: Maximum value distribution of grating lobe

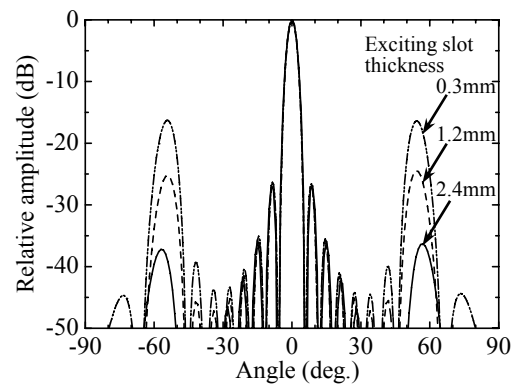


Figure 10: Improvement of radiation pattern

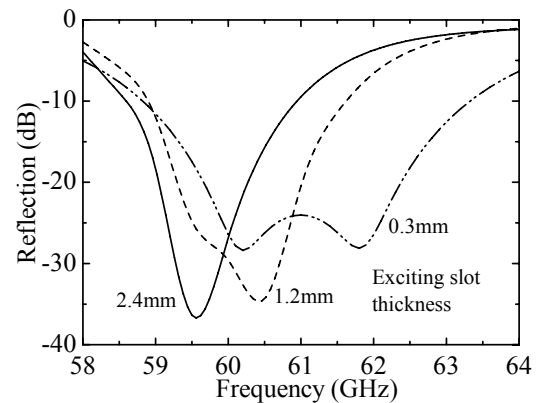


Figure 11: Degradation of reflection characteristic